Supporting Information

High performance intensiometric direct- and inverse-response genetically encoded biosensors for citrate

Yufeng Zhao[1], Yi Shen[1], Yurong Wen[2*], and Robert E. Campbell[1,3*]

[1]Department of Chemistry, University of Alberta, Edmonton, Alberta, Canada

[2]Department of Talent Highland, The First Affiliated Hospital, Xi'an Jiaotong University, Xi'an, Shaanxi, China

[3]Department of Chemistry, Graduate School of Science, The University of Tokyo, Tokyo, Japan

*Correspondence regarding x-ray crystallography should be addressed to Y.W. (yurong.wen@xjtu.edu.cn). All other correspondence should be addressed to R.E.C. (robert.e.campbell@ualberta.ca)

Methods

Plasmid construction

A pBAD/HisB (Thermo Fisher Scientific) plasmid containing the gene for ncpGCAMP6 was used as the template and amplified by PCR using Q5 polymerase to prepare the vector containing ncpGFP[27]. A synthetic gene (gBlocks) for CitAP and overlap regions with the vector for assembly was purchased from Integrated DNA Technologies. The CitAP gene was cloned into the vector using Gibson assembly (New England Biolabs) and the resulting plasmid was used to transform DH10B electrocompetent cells. Plasmids were purified from 4 mL liquid culture of a single colony using the GeneJET miniprep kit and verified by sequencing.

Linker optimization, directed evolution and K_d tuning

The two linkers were optimized separately using Quikchange II site-directed mutagenesis Lightening kit (Agilent) with customized primers. *E. coli* was transformed with gene libraries in the context of pBAD/HisB plasmids. Colonies showing high fluorescence intensity were picked and cultured in liquid media, followed by protein extraction with B-PER (Bacterial Protein Extraction Reagent, ThermoFisher Scientific), and fluorescence measurement in plate reader. A directed evolution strategy was employed to improve the dynamic range of the biosensors after linker optimization. Libraries were created using error-prone PCR as previously described[59]. In the first round of screening, ~25 colonies out of ~5000 colonies on agar plates were picked and cultured in 4 mL media using 15 mL culture tubes (Falcon). For the following rounds of directed evolution, 96 well culture blocks (Corning) were used for 1 mL liquid culture for higher-throughput screening (100 - 500 out of ~5000 colonies per round). Overnight cultures were spun down in centrifuge to pellet the bacteria, and B-PER was used to extract proteins for fluorescence measurement. Site-directed mutagenesis at single and double positions was utilized to change the citrate binding affinity. For screening purposes, each

variant extracted from bacteria was tested in TBS buffer with 0.02, 0.2, 2 and 20 mM citrate.

Protein purification and in vitro characterization

To purify the citrate biosensors for *in vitro* characterization, we first used the pBAD plasmids containing the gene encoding citrate biosensors to transform DH10B electrocompetent cells. Bacteria were then plated on LB-agar plates with 400 μg/mL ampicillin and 0.02% (wt/vol) arabinose for overnight incubation at 37 ℃. The following day, colonies were picked and sub-cultured in 500 mL LB media containing 400 μg/mL ampicillin in a shaker at 37 ℃ for 24 h. The media was then supplemented with 0.02% (wt/vol) arabinose and shaken at room temperature for another 24 h. Bacterial cells were harvested using centrifuge and re-suspended in 50 mL Tris-buffered saline (TBS). The cells were lysed using sonication and the supernatant was obtained after centrifugation at 13,000 *g* for 30 min. The protein biosensors were purified by Ni-NTA agarose (MCLAB) and the TBS buffer was exchanged into MOPS buffer using 10 kDa ultrafiltration tubes (Amicon).

A Beckman DU-800 UV-vis spectrophotometer was used to measure absorption spectra and a Tecan Safire2 fluorescence plate reader was used to measure the excitation and emission fluorescence spectra. Extinction coefficient and quantum yield of each variant in the bound and unbound state was measured and calculated as previously described[60]. The brightness of the biosensor was determined as the product of extinction coefficient and quantum yield. To measure the binding affinity, proteins were diluted in various MOPS buffer containing citrate at the concentration ranging from 1 μM to 50 mM for fluorescence measurement. The fluorescence vs. concentration of citrate was plotted and fitted in Origin using Hill equation for determination of apparent K_d. pH profiles of the proteins were similarly acquired. Proteins were diluted in a series of buffer with 30 mM sodium acetate and 30 mM borax (pH ranges from 4.5 to 11) for fluorescence measurement. Fluorescence vs. pH of the biosensor at bound and

unbound state was plotted. For specificity test, the fluorescence spectra of each biosensor variant in MOPS buffer with or without 20 mM metabolite (citrate, malate, fumarate, succinate or α-ketoglutarate) were acquired.

Crystallization and structure determination

The Citron1 recombinant protein was further purified with size exclusion chromatography using Superdex200 column (GE) in 20 mM Tris pH 8.0, 150 mM NaCl supplemented with 100 mM sodium citrate, and concentrated to 15 mg/mL for crystallization trials. The initial crystallization screen was carried out with 384-well plates (Molecular Dimensions) via sitting drop vapor diffusion against commercial sparse matrix screen kit (Hampton) at 20 °C. The recombinant Citron1 protein was crystallized in 4% v/v tacsimate pH 5.0, 12% w/v polyethylene glycol 3350. The Citron1 crystal was cryoprotected with the reservoir solution in supplement with 20% glycerol and flash frozen in liquid nitrogen. The dataset was collected in Shanghai Synchrotron Radiation Facility Beamline BL19U1 with wavelength of 0.98 Å and the X-ray diffraction data were processed and scaled with XDS package[61]. The data collection details and statistics are summarized in **Table S3**.

The Citron1 structure was solved with molecular replacement using both the GFP (6GEL) and CitA citrate-binding domain (2J80) as search model[25,62]. The density of the linker and citrate ions were observed after initial refinement, the manual model building of the missing residues and further refinement were carried out with COOT and PHENIX suite [63,64]. The Citron1 in complex with citrate was solved at a resolution of 2.99 Å in the unit cell of a = b = 92.4 Å, c = 123.0 Å, and refined with a R_{work} of 0.2227 and R_{free} factor of 0.2822, respectively. The final Citron1 model contains two monomers and includes residues ranging from 2-361, 2 citrate ions and some residues from the cloning tag sequence. The structure exhibited good stereochemistry and showed a favorable Ramachandran plot. Detailed

refinement statistics are provided in **Table S3**. Structure coordinates have been deposited in the Protein Data Bank with a code of 6LNP.

HeLa cell imaging

The genes encoding the citrate biosensors were digested with XhoI and HindIII, and ligated into pcDNA3.1 (Thermo Fisher Scientific) vectors for cytoplasmic expression in mammalian cells. For mitochondria-targeting, genes of interest were amplified using Q5 PCR, purified, digested with BamH1 and HindIII, and ligated into a similarly-digested pcDNA3.1 vector with mitochondria-targeting sequence from cytochrome C oxidase signal peptide (MSVLTPLLLRGLTGSARRLPVPRAKIHSLGDP). Constructed plasmids were used to transform *E. coli* cells for plasmid amplification and purification with miniprep kits. HeLa cells were cultured in DMEM media with 10% fetal bovine serum and penicillin-streptomycin (Thermo Fisher Scientific). Cells were plated in either 35 mm glass bottom dishes or 24-well glass bottom plates, transfected using Turbofect (Thermo Fisher Scientific) according to the protocols provided in the manual, and incubated in a CO_2 incubator for 24 - 48 h. Before imaging, cell culture media was removed and cells were washed twice with phosphate buffered saline (PBS), which was then replaced with HEPES buffered HBSS solution for imaging. Cell culture dishes or plates were fixed on the stage of a Nikon Eclipse Ti-E microscope or a Zeiss Axiovert 200 microscope with a 20× objective. Software was used to control the microscopes (NIS-Elements Advanced Research (Nikon) for the Nikon microscope and MetaMorph (Molecular Devices) for the Zeiss microscope). A GFP optical filter set (470/40 nm excitation and 525/50 nm emission) was used for imaging the citrate biosensors. The GFP filter set and an RFP optical filter set (535/50 nm excitation and 609/57 nm emission) was used and alternatively switched for dual-color imaging of the green citrate biosensors and the red ATP biosensor MalionR[43].

For cell permeabilization experiments, time-lapse images were acquired every 10 or 20 s with appropriate exposure. Digitonin solution (0.1%) was added to reach a concentration of 0.0005% for plasma membrane permeabilization and 0.005% for mitochondrial membrane permeabilization after the imaging was initiated for ~100 s. A stock citrate solution (0.5 M) was then added to reach a concentration of 10 mM after the imaging was initiated for ~400 s. For *in situ* titration, cells were similarly permeabilized and various amounts of citrate solution were added to the buffer. After each citrate addition, cells were imaged for ~400 s to allow them to equilibrate and for the fluorescence to stabilize before the next addition.

To image pharmacologically-induced citrate concentration changes (with glucose, BMS-303141 or UK-5099), time-lapse images were acquired every 10 s to 10 min, with appropriate exposure times. For imaging of glucose treatment, cells were first starved in a glucose-free buffer for ~0.5 - 1 h before imaging. A solution of 500 mM glucose, 100 μM BMS-303141 or 1 mM UK-5099 was added to the imaging buffer to reach a final concentration of 20 mM for glucose, 5 μM for BMS-303141 or 25 μM for UK-5099, at about 2 min after the imaging was initiated. Due to the limited solubility in aqueous phase, UK-5099 was first dissolved in DMSO and then diluted with water. This resulted in a relatively high concentration of DMSO, a final concentration of ~0.25% (vol/vol) being added to the imaging buffer together with UK-5099. For control experiments, the same concentration of DMSO solution was used to treat HeLa cells expressing either Citron1 or CitronRH. Representative traces for cell imaging experiments are provided in **Fig. S14**.

For dual color imaging of citrate and ATP concentration changes in mitochondria, the gene encoding MalionR (Addgene plasmid #113908) was amplified by PCR, digested with BamH1 and HindIII, and cloned into the mitochondria-targeting vector. An approximately 1:1 mixture of plasmids of mitochondria-targeted Citron1 and MalionR were used to co-transfect HeLa cells using the protocol described above. After 24 h incubation, cells were starved in a

glucose free buffer for 0.5 - 1.0 h and then imaged. Glucose was added to induce citrate/ATP changes while imaging.

INS-1 cell imaging

INS-1 cells were cultured in RPMI-1640 (Invitrogen) supplemented with 10% fetal bovine serum, 1% penicillin-streptomycin, 10 mM HEPES, 1 mM sodium pyruvate, 2 mM L-glutamine and 50 μM β-mercaptoethanol at 37 ℃ in a CO_2 incubator. Cells were plated in 24-well glass bottom plates, and transfected using Lipofectamine 2000 (Invitrogen) according to the manual. Plasmids used for cytosolic and mitochondrial expression were the same as those used for HeLa cells. Before imaging, the culture medium was removed, INS-1 cells were washed twice with PBS buffer and Krebs-Ringer buffer (PH 7.4) was used for imaging. Krebs-Ringer buffer contains 0.1% BSA, 10 mM HEPES, 115 mM NaCl, 5 mM KCl, 24 mM $NaHCO_3$, 2.5 mM $CaCl_2$, and 1 mM $MgCl_2$. Imaging was performed on a Nikon Eclipse Ti-E microscope or a Zeiss Axiovert 200M microscope. Citrate concentration in the cytosol or mitochondria was quantified similarly as HeLa cell experiments using *in situ* titration. To stimulate intracellular citrate changes, 20 mM glucose or 2 mM 1,2,3-benzenetricarboxylate (BTC) was added to the imaging buffer and the corresponding citrate concentration changes were tracked with Citron1.

Safety statement

No unexpected or unusually high safety hazards were encountered.

Supplementary Tables

Table S1. *In vitro* characterization of Citron1 and Citroff1.

Biosensor	**State**	**Extinction coefficient ($mM^{-1}cm^{-1}$)**	**Quantum yield**	**Brightness[1]**	**K_d**	**$\Delta F/F_{min}$[2]**
Citron1	+ citrate	61.6	0.34	21	1.1 mM	9
	- citrate	7.2	0.29	2.1		
Citroff1	+ citrate	3.0	0.44	1.3	5 μM	19
	- citrate	66.8	0.38	25		

[1] Brightness = extinction coefficient × quantum yield.

[2] For Citron1, $\Delta F/F_{min} = F_{+citrate} - F_{-citrate} / F_{-citrate}$. For Citroff1, $\Delta F/F_{min} = F_{-citrate} - F_{+citrate} / F_{+citrate}$.

Table S2. Summary of K_d and dynamic range of Citron1 and Citroff1 variants.

Variant	**K_d (μM)**	**$\Delta F/F_{min}$**
Citron1	1100	9
Citroff1	5	19
Citroff1 S244A	35	20
Citroff1 R250A	153	17
Citroff1 S244A Y199F	965	11

Table S3. X-ray data collection and refinement statistics. Statistics for the highest resolution shell are shown in parentheses.

Crystal	Citron1
Data collection	
Spacegroup	P 41
a, b, c (Å)	92.4, 92.4, 123.0
α, β, γ (°)	90°, 90°, 90°
Resolution (Å)	44.79-2.99 (3.10-2.99)
*R*merge	0.134 (1.37)
*R*meas	0.143 (1.46)
Multiplicity	13.6 (14.2)
CC(1/2)	0.998 (0.65)
CC*	0.999 (0.887)
I/σ(I)	12.1 (1.1)
Completeness (%)	99.76 (99.86)
Wilson B-factor (Å^2)	52.55
Refinement	
Total Reflections	284653 (29409)
Unique Reflections	20881 (2072)
R_{work}/R_{free}	0.2227/0.2822
Number of atoms:	
Protein	5518
Ligands	70
Protein Residues	733
Average B-factor (Å^2)	51.33
Protein ADP (Å^2)	51.29
Ligands (Å^2)	54.52
Ramachandran plot:	
Favored/Allowed (%)	92.1/7.5
Root-Mean-Square-Deviation:	
Bond lengths (Å)	0.004
Bond Angle (°)	0.80
PDB code	6LNP

Supplementary Figures

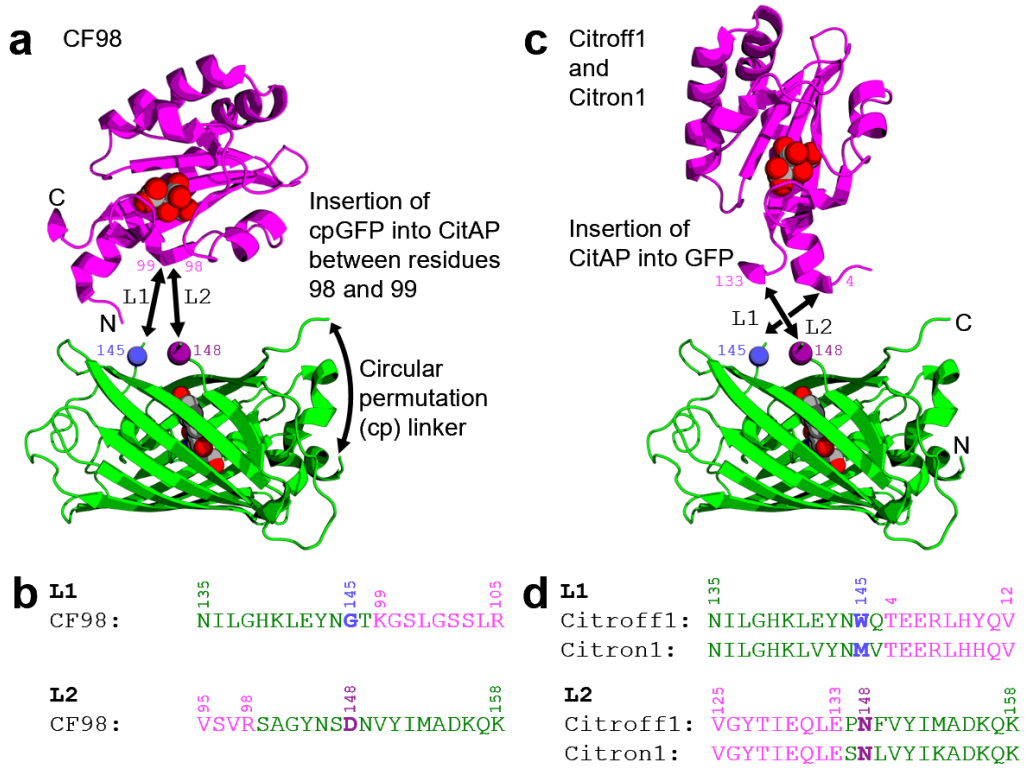

Figure S1 Comparison of the design of the previously reported CF98 biosensor and the design of the Citroff1 and Citron1 biosensors described in this work. Residues are numbered according to the original CitAP and GFP sequences. **a** CF98 was designed based on the rationale of propagating the binding-induced conformational change in the minor loop of CitAP (refer to **Fig. 1b**) into a change in the GFP chromophore environment[28]. To realize this design, cpGFP was inserted into the minor loop between residues 98 and 99. The CitAP domain with bound citrate is shown in magenta (PDB ID 2J80)[25] and the GFP domain from GCaMP6m is shown in green (PDB ID 3WLD)[65]. Residues 145 (Cα represented as blue sphere) and 148 (Cα represented as a purple sphere) are shown as reference points. Black arrows are used to represent the linkage from GFP to residue 99 of CitAP (L1), the linkage from residue 98 of CitAP to GFP

(L2), and the cp linker that connects the original N- and C-termini (which was disordered and not observed in this structure). **b** Sequences in the vicinity of the L1 and L2 connections between GFP and CitAP in the CF98 biosensor. Residues 145 and 148 are colored as in **a**. **c** In this work we describe citrate biosensors based on the rationale of propagating the binding induced conformational changes at the C-terminus of CitAP (refer to **Fig. 1**) into a change in the GFP chromophore environment. To realize this design, the CitAP domain was inserted into GFP at the same site where CaM-RS20 is inserted in the ncpGCaMP6s[27] biosensor (a topological variant of GCaMP6s)[36]. Protein structures are represented as in **a**. L1 is the connection between GFP and residue 4 of CitAP, and L2 is the connection between residue 133 of CitAP and GFP, and there is no cp linker in this design. **d** Sequences in the vicinity of L1 and L2 for the Citroff1 and Citron1 biosensors. Residues 145 and 148 are colored as in **c**.

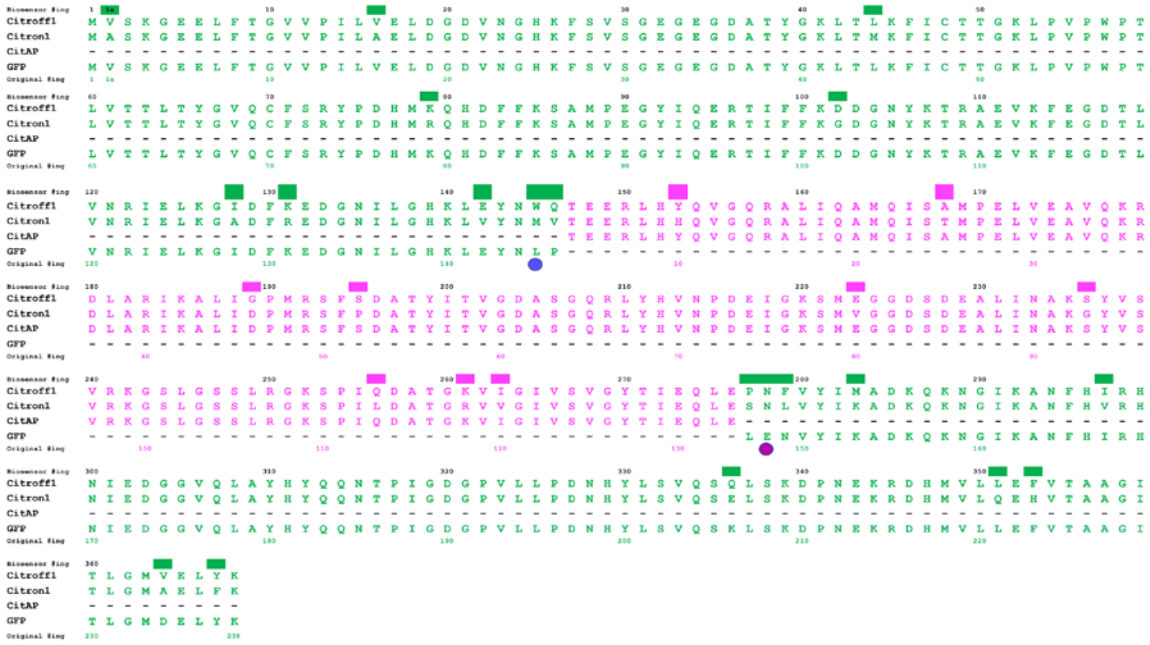

Figure S2 Sequence alignment of citrate biosensors described in this work. The CitAP sequence (magenta) is from, and numbered (bottom) as in, PDB ID 2J80[25]. The GFP sequence (green) is from ncpGCaMPs[27] and numbered (bottom) according to wild-type GFP[66]. Numbers at the top correspond to residue numbering for the full length biosensors. The positions of mutations accumulated during biosensor optimization are represented with colored bars over the position of the mutation. Relative to the starting template sequences, Citroff1 acquired 5 mutations in linker regions, 3 mutations in GFP, and 1 mutation in CitA. Citron1 acquired 5 mutations in linker regions, 14 mutations in GFP, and 8 mutations in CitA.

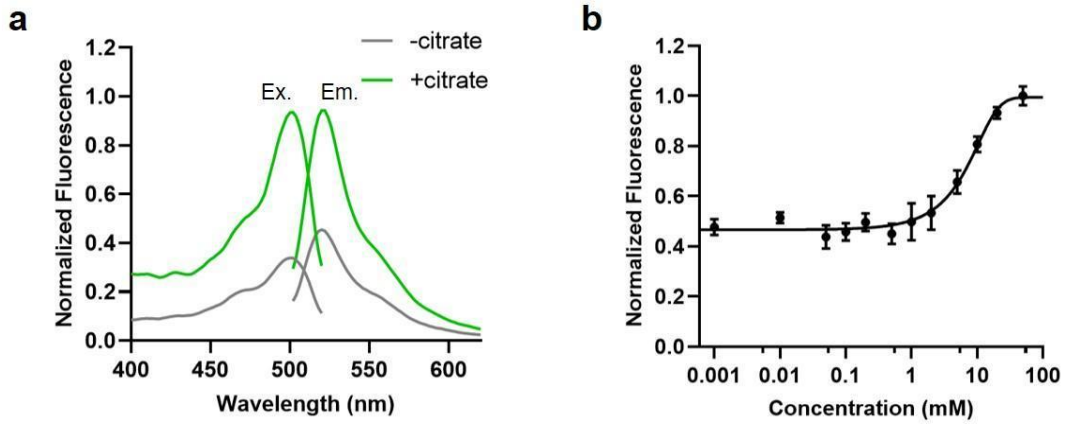

Figure S3 *In vitro* characterization of CF98. **a** Normalized excitation and emission spectra of purified CF98. **b** *In vitro* citrate titration curve of purified CF98. Error bars represent the standard deviation of triplicates.

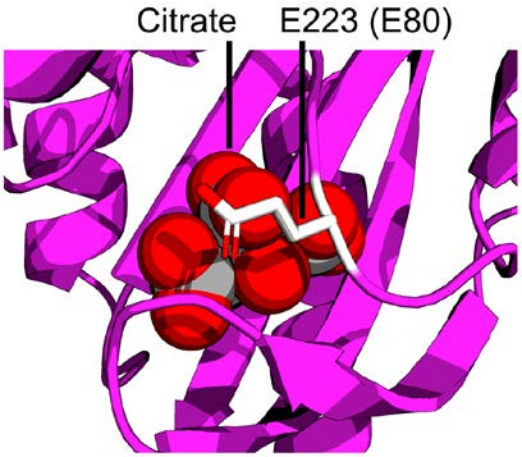

Figure S4 Location of the E223V mutation (equivalent to E80V as numbered in PDB ID 2J80)[25] in Citron1.

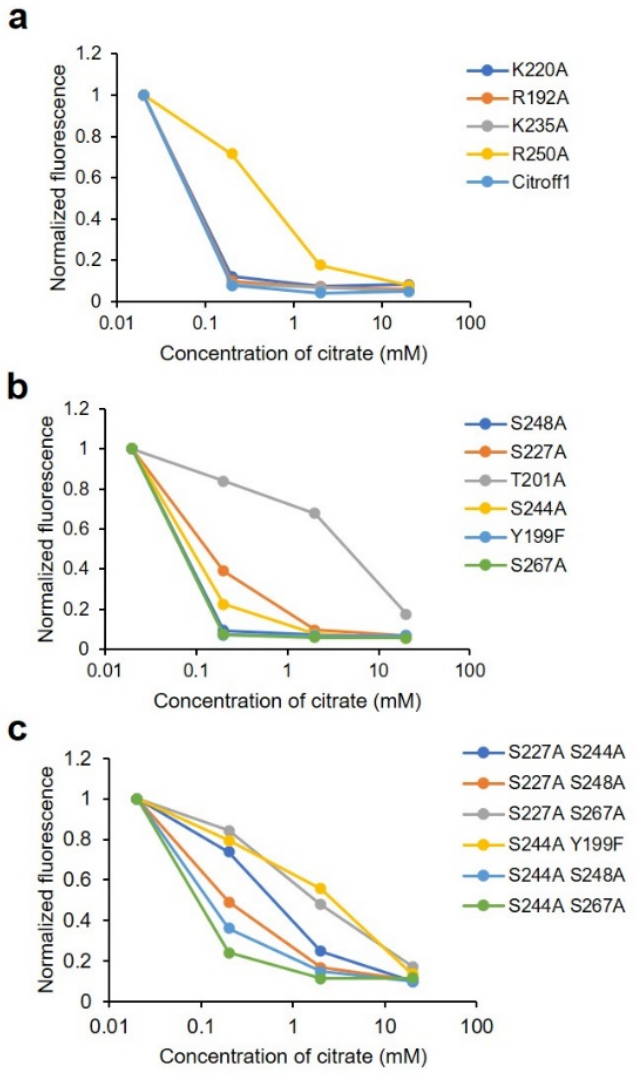

Figure S5 Introduction of mutations to decrease the binding affinity of Citroff1. **a** Introduction of mutations that were previously reported to decrease the affinity of a CitAP-based biosensor[28]. **b** Introduction of various structure-guided mutations that were hypothesized to potentially decrease the affinity for citrate. **c** Pairwise combinations of mutations.

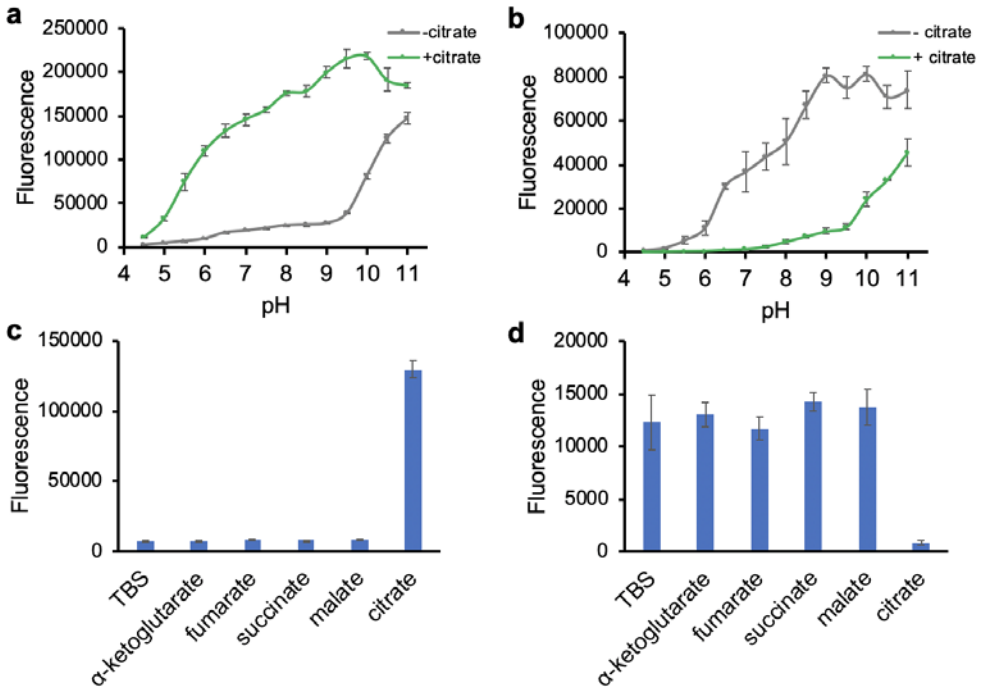

Figure S6 pH dependence and specificity of citrate biosensors. **a,b** Fluorescence response of Citron1 (**a**) and Citroff1 (**b**) at various pH values with or without 20 mM Citrate. **c,d** Specificity of Citron1 (**c**) and Citroff1 (**d**) to various metabolites (20 mM each metabolite in TBS buffer). Error bars represent the standard deviation of triplicates.

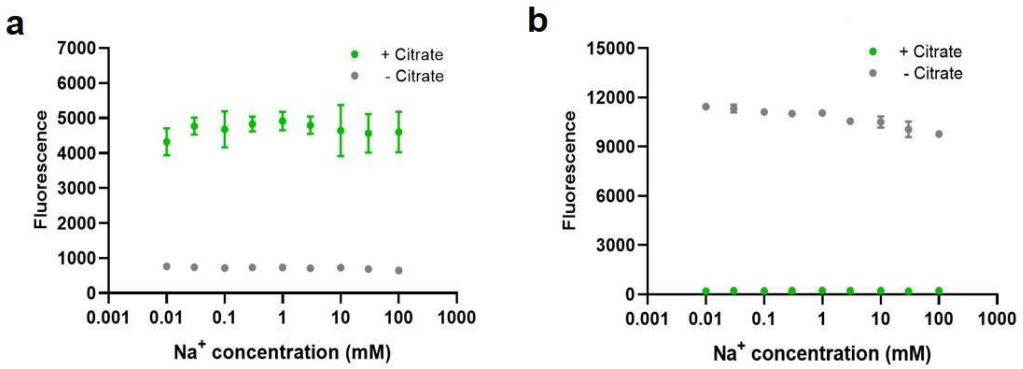

Figure S7 Na^+ concentration dependence of Citron1 (**a**) and Citroff1 (**b**), with 30 mM citrate in the + citrate condition. Error bars represent the standard deviation of triplicates.

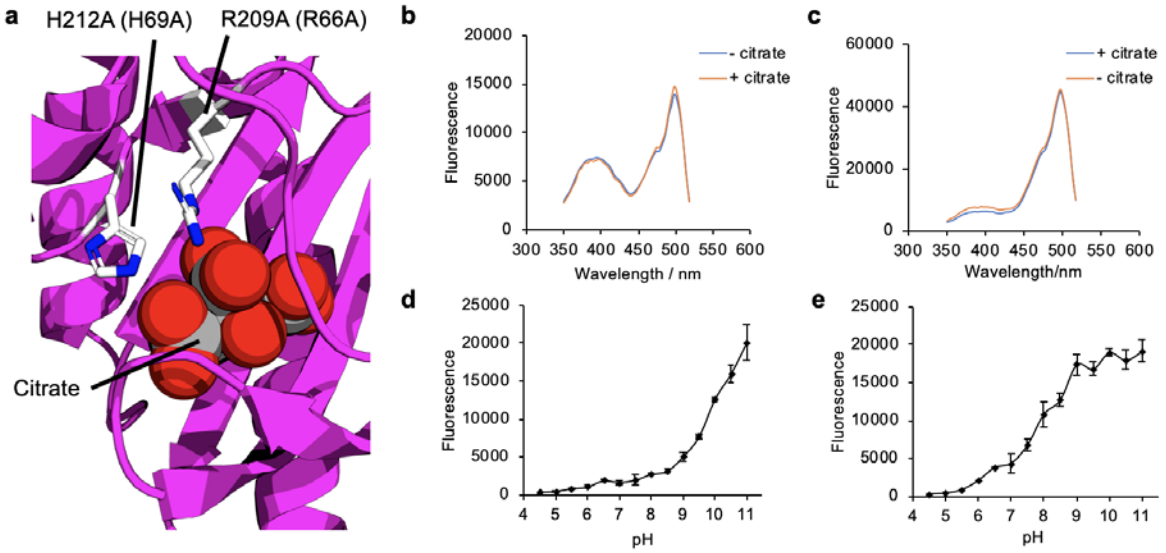

Figure S8 Engineering citrate-insensitive control constructs. **a** Crystal structure of CitAP (PDB ID 2J80)[25] with side chains of H212 and R209 (biosensor numbering, equivalent to H69 and R66 of CitAP) shown in stick representation. Mutation of these two residues to alanine was sufficient to disable citrate binding. **b,c** Excitation spectra of control variants CitronRH (**b**) and CitroffRH (**a**) with or without citrate in the buffer. **d,e** pH profiles of CitronRH (**d**) and CitroffRH (**e**). Error bars represent the standard deviation of triplicates.

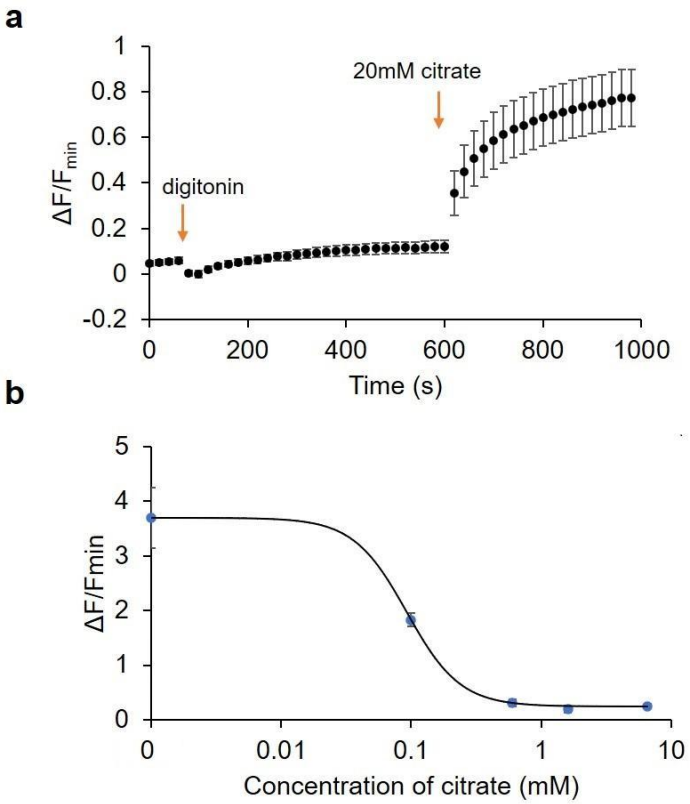

Figure S9 Additional information related to *in situ* calibration of citrate biosensors. **a** Citron1 expressed in the mitochondria of HeLa cells in response to digitonin and citrate (n = 22). **b** *In situ* titration curve of Citroff1 in the cytosol (n = 26). Error bars represent s.e.m..

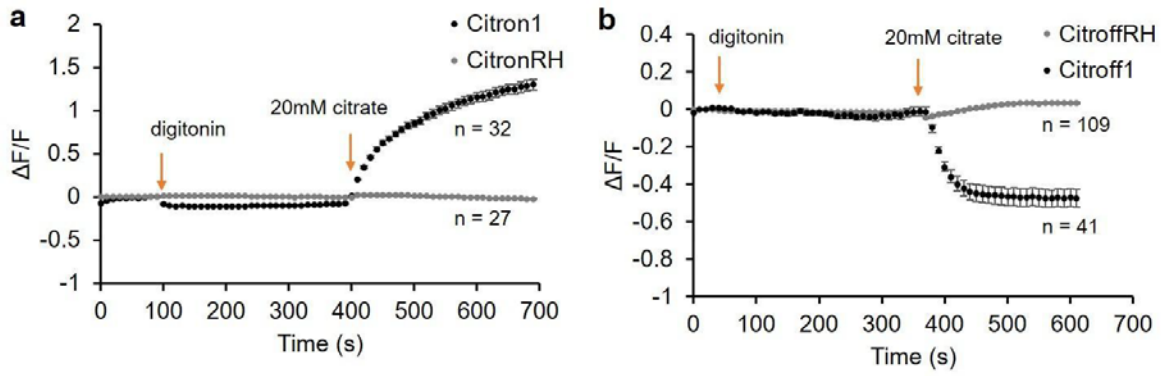

Figure S10 Comparison of citrate biosensors (Citron1 and Citroff1) and control variants (CitronRH and CitroffRH) expressed in the cytosol. Cells were treated with digitonin and citrate. Error bars represent s.e.m..

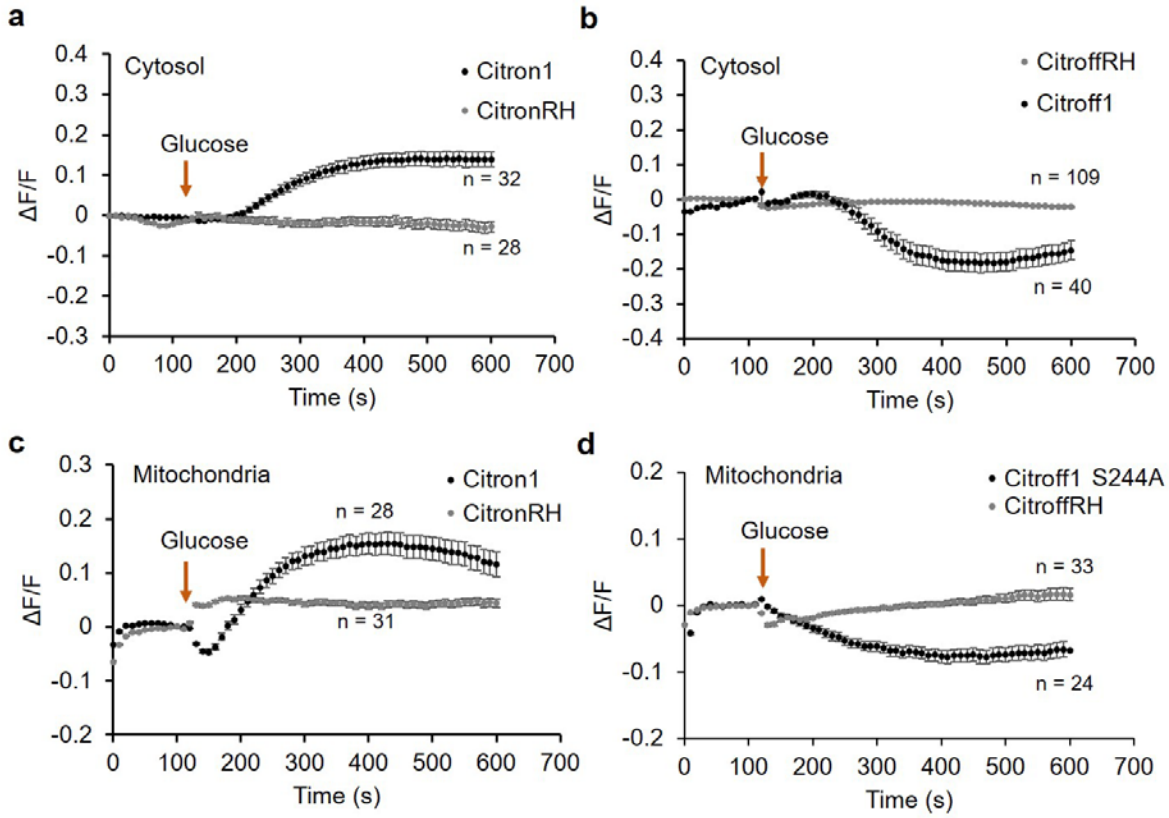

Figure S11 Responses of citrate biosensors (Citron1 and Citroff1 variant) and control variants (CitronRH and CitroffRH) expressed in the cytosol (**a**,**b**) and mitochondria (**c**,**d**) of HeLa cells during treatment with glucose. Error bars represent s.e.m..

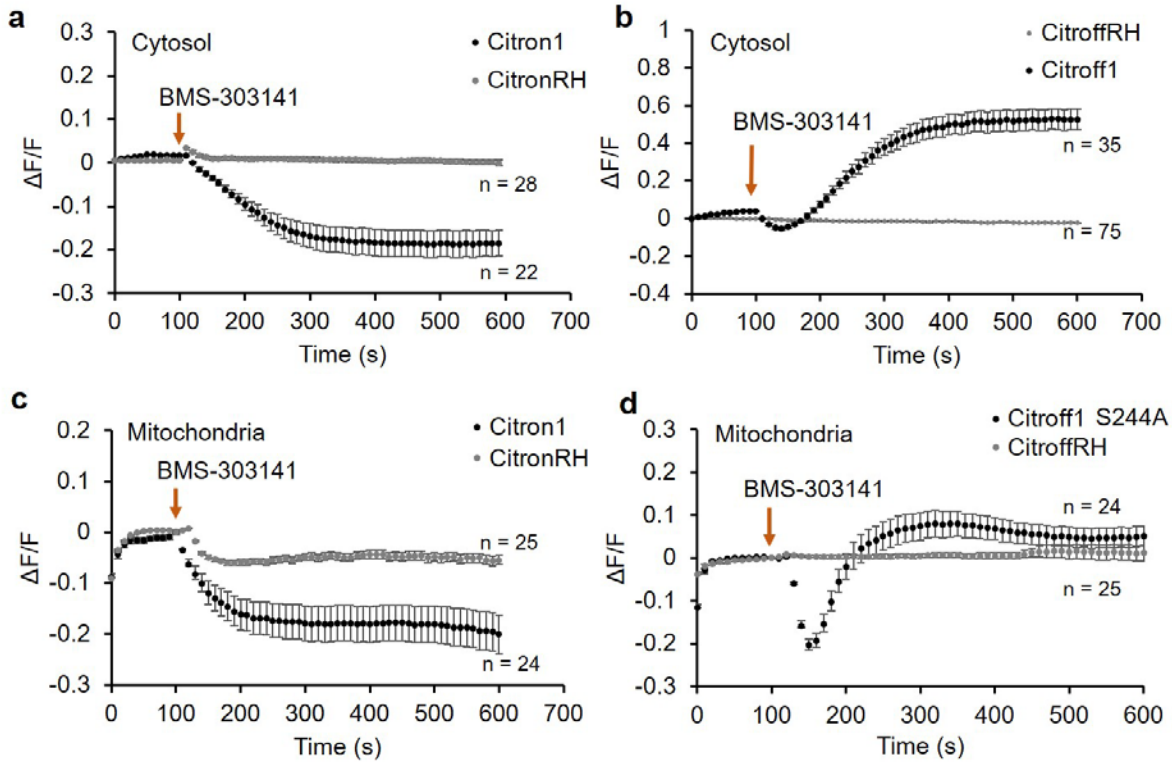

Figure S12 Comparison of citrate biosensors (Citron1 and Citroff1 variant) and control variants (CitronRH and CitroffRH) expressed in the cytosol (**a**,**b**) and mitochondria (**c**,**d**) during treatment with BMS-303141. Error bars represent s.e.m..

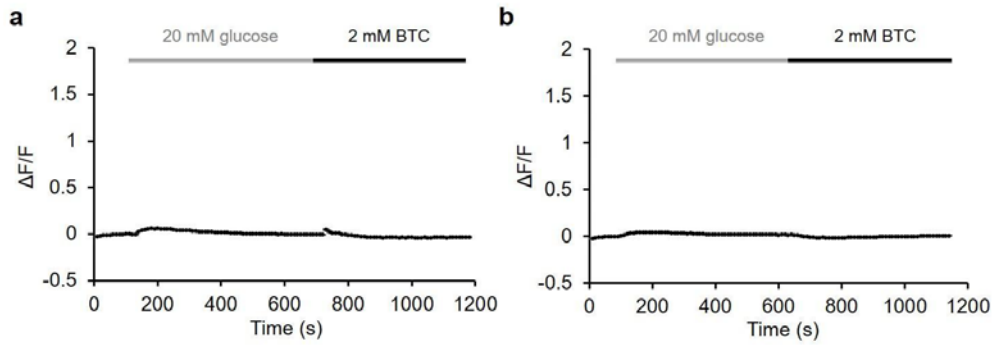

Figure S13 Imaging of the non-binding CitronRH variant in the cytosol (**a**, n = 23) and mitochondria (**b**, n = 16) of INS-1 cells. Cells were treated with 20 mM glucose and 2 mM BTC as indicated. Y-axis range is scaled to match **Fig. 5e**. Error bars represent s.e.m..

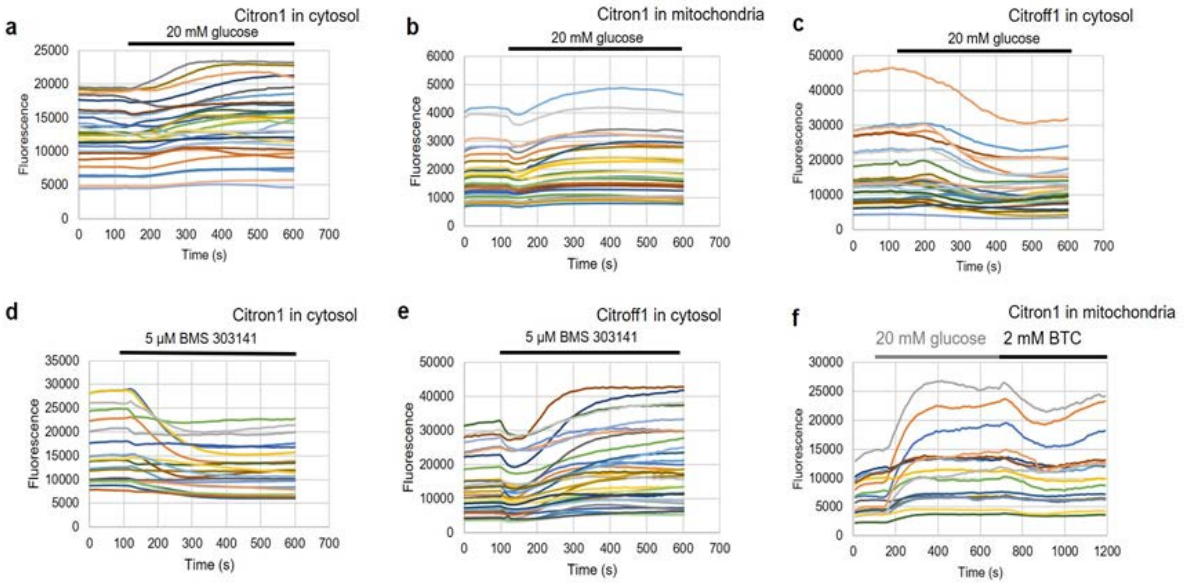

Figure S14 Examples of fluorescence traces of citrate biosensors from individual cells upon perturbation. **a**-**c** Glucose-induced citrate change in HeLa cells revealed by Citron1 in cytosol (**a**), Citron1 in mitochondria (**b**) and Citroff1 in cytosol (**c**). Processed data of **a**, **b,** and **c** are shown in **Fig. 4a** (orange curve), **Fig. 4a** (green curve), and **Fig. S11b**, respectively. **d**-**e** BMS-303141-induced citrate change in HeLa cells revealed by Citron1 (**d**) and Citroff1 (**e**) in cytosol. **f** Glucose- and BTC-induced citrate changes in INS1 cells revealed by Citron1 in cytosol. Processed data of **d**, **e**, and **f** are shown in **Fig. 4b**, **Fig. S12b,** and **Fig. 5f**, respectively.

Data availability

The data supporting this research are available upon request. Structure coordinates have been deposited in the Protein Data Bank with a code of 6LNP. Plasmid constructs encoding Citron1(#134300, #134303, #134305), Citroff1 (#134301, #134304), and other affinity variants (#134302, #134306, #134307) are available through Addgene.

Supplementary Reference

1. Qian, Y., Rancic, V., Wu, J., Ballanyi, K. & Campbell, R. E. A Bioluminescent Ca2+ Indicator Based on a Topological Variant of GCaMP6s. *Chembiochem* **20**, 516–520 (2019).
2. Zhao, Y. *et al.* Microfluidic cell sorter-aided directed evolution of a protein-based calcium ion indicator with an inverted fluorescent response. *Integr. Biol.* **6**, 714–725 (2014).
3. Shen, Y. *et al.* Genetically encoded fluorescent indicators for imaging intracellular potassium ion concentration. *Commun. Biol.* **2**, 18 (2019).
4. Kabsch, W. XDS. *Acta Crystallogr. D Biol. Crystallogr.* **66**, 125–132 (2010).
5. Trigo-Mourino, P., Thestrup, T., Griesbeck, O., Griesinger, C. & Becker, S. Dynamic tuning of FRET in a green fluorescent protein biosensor. *Sci. Adv.* **5**, eaaw4988 (2019).
6. Sevvana, M. *et al.* A ligand-induced switch in the periplasmic domain of sensor histidine kinase CitA. *J. Mol. Biol.* **377**, 512–523 (2008).
7. Emsley, P., Lohkamp, B., Scott, W. G. & Cowtan, K. Features and development of Coot. *Acta Crystallogr. D Biol. Crystallogr.* **66**, 486–501 (2010).
8. Adams, P. D. *et al.* PHENIX: a comprehensive Python-based system for macromolecular structure solution. *Acta Crystallogr. D Biol. Crystallogr.* **66**, 213–221 (2010).
9. Arai, S. *et al.* RGB-Color Intensiometric Indicators to Visualize Spatiotemporal Dynamics of ATP in Single Cells. *Angew. Chem. Int. Ed.* **57**, 10873–10878 (2018).
10. Honda, Y. & Kirimura, K. Generation of circularly permuted fluorescent-protein-based indicators for in vitro and in vivo detection of citrate. *PLoS One* **8**, e64597 (2013).
11. Ding, J., Luo, A. F., Hu, L., Wang, D. & Shao, F. Structural basis of the ultrasensitive calcium indicator GCaMP6. *Sci. China Life Sci.* **57**, 269–274 (2014).
12. Chen, T.-W. *et al.* Ultrasensitive fluorescent proteins for imaging neuronal activity. *Nature* **499**, 295–300 (2013).
13. Tsien, R. Y. The green fluorescent protein. *Annu. Rev. Biochem.* **67**, 509–544 (1998).